Physics of the Solid State, Vol. 45, No. 10, 2003, pp. 1866–1873. Translated from Fizika Tverdogo Tela, Vol. 45, No. 10, 2003, pp. 1776–1783.

METALS AND SUPERCONDUCTORS

Transport and Magnetic Properties of $Y_{3/4}Lu_{1/4}Ba_2Cu_3O_7 + Y_3Fe_5O_{12}$ Composites Representing a Josephson-Type Superconductor–Ferrimagnet–Superconductor Weak-Link Network

K. A. Shaĭkhutdinov, D. A. Balaev, S. I. Popkov, and M. I. Petrov

Kirensky Institute of Physics, Siberian Division, Russian Academy of Sciences, Akademgorodok, Krasnoyarsk, 660036 Russia

e-mail: smp@iph.krasn.ru

Received February 25, 2003

Abstract—$Y_{3/4}Lu_{1/4}Ba_2Cu_3O_7 + Y_3Fe_5O_{12}$ composites with different volume ratios of the starting components were synthesized. The composites model an S–F–S Josephson junction network, where S stands for a superconductor and F, for a ferrimagnet. A study of the transport characteristics of the composites revealed that the temperature behavior of the electrical resistivity $\rho(T)$ below the superconducting transition point T_C is different in two regions separated by a temperature T_m. Below T_m, the current–voltage characteristics of the composites are nonlinear, while in the interval from T_C to T_m the values of $\rho(T)$ do not depend on the transport current j and magnetic field H. This behavior of $\rho(T, j)$ and $\rho(T, H)$ is assigned to specific features of the tunneling of superconducting carriers through the ferrimagnetic layers separating HTSC grains in the composite. Magnetic measurements showed the diamagnetic response of HTSC grains to be lower in composites with a ferrimagnet. © *2003 MAIK "Nauka/Interperiodica".*

1. INTRODUCTION

Two-phase composite materials based on high-temperature superconductors (HTSCs) are of considerable interest from both a practical [1–8] and a scientific [2, 3, 5, 6, 9–14] viewpoint. The latter is due to these objects representing a Josephson-coupled weak-link network. The second, nonsuperconducting, component of the composite (insulator, semiconductor, normal metal) acts as an artificially created weak link between HTSC grains. By properly varying the volume concentration ratio of the starting components in such composites, one can vary the effective extent (or "strength") of the weak link within a broad range.

Obviously enough, a single Josephson junction would be an ideal object for investigation, but the small coherence length and the strong chemical reactivity of HTSCs make fabrication and study of such structures a difficult task. However, as shown earlier [10, 11, 14, 15], the transport characteristics (the temperature dependences of electrical resistivity $\rho(T)$ and of the critical current $j_C(T)$, the current–voltage curves) of HTSC-based two-phase composite materials reflect the main features of superconducting carrier flow through a single Josephson junction of a certain effective extension in space, while the relative simplicity of fabrication of such materials makes them attractive objects for studies and for possible applications [7, 8].

We recently studied the transport properties of composites with magnetic impurities in a nonsuperconducting composite (HTSC + $Cu_{1-x}Ni_xO$ ($0 < x < 0.06$) [15], HTSC + $BaPb_{0.9}Fe_{0.1}O_3$, HTSC + $BaPb_{0.9}Ni_{0.1}O_3$ [16]) and found that the superconducting properties of such composites are strongly suppressed by the interaction of the spins of superconducting carriers with magnetic moments during their crossing of the nonsuperconducting layer. Investigation of the transport properties of the composite HTSC + paramagnetic insulator ($NiTiO_3$) [17, 18] revealed not only a strong suppression of superconducting properties but also an anomalous behavior of the temperature dependences of electrical resistivity. Within the temperature interval from the onset of the superconducting transition in the HTSC grains (at T_C) to a certain temperature T_m, the electrical resistivity does not depend on the magnitude of the transport current and applied magnetic field (the I–V curves are linear) and becomes a function of these quantities only below T_m, a feature characteristic of Josephson-type weak links. This anomalous behavior of the temperature dependence of electrical resistivity of the HTSC + $NiTiO_3$ composites was attributed to exchange interaction of superconducting-carrier spins with the magnetic moments of nickel in the paramagnetic phase. This interaction results in an anomaly in the temperature behavior of electrical resistivity at the melting temperature of the Abrikosov vortex lattice in HTSC grains [17, 18].

The next step in investigating composites with magnetically active nonsuperconducting components was a study of HTSC + ferrimagnet composites. Single S–F–S structures (S stands for a superconductor, and F, for a

ferro- or ferrimagnet) have become a subject of intense current research, both theoretical [19–26] and experimental [27–29], because they exhibit interesting phenomena, such as a nonmonotonic dependence of the critical current on temperature [25], a manifestation of π coupling [19, 24, 25], a reduction of superconducting properties, and a characteristic behavior of magnetoresistance [27]. Of the large family of ferro- and ferrimagnetic compounds, we chose $Y_3Fe_5O_{12}$ (classical yttrium–iron garnet), an insulator which interacts weakly enough with the 1-2-3 HTSC structure. To establish the effect of ferrimagnetic ordering in the insulating spacer on the transport properties of composites, we also prepared and studied HTSC + $Y_3Al_5O_{12}$ reference composites, because the $Y_3Al_5O_{12}$ compound is isostructural to $Y_3Fe_5O_{12}$ and nonmagnetic.

2. EXPERIMENTAL

The $Y_{3/4}Lu_{1/4}Ba_2Cu_3O_7$ polycrystalline HTSC was prepared using standard ceramic technology. The nonsuperconducting components of the composites, namely, $Y_3Fe_5O_{12}$ and $Y_3Al_5O_{12}$, were synthesized from Y_2O_3 and Fe_3O_4, $Al(OH)_3$, accordingly, at a temperature of 1250°C for 48 h with three intermediate grindings. After that, the starting components of the composites to be obtained were taken in correct proportion, ground thoroughly in an agate mortar, and pelletized. The pellets were put into preliminarily heated boats and placed in a furnace heated to 910°C for 2 min. They were subsequently kept in another furnace for 3 h at t = 350°C and cooled with the furnace. This method of rapid sintering [11] was employed to prepare composite samples with different volume contents of the HTSC and nonsuperconducting components $Y_3Fe_5O_{12}$ and $Y_3Al_5O_{12}$. We denote our composite materials by S + *V*YIG and S + *V*YAlG, where S stands for the $Y_{3/4}Lu_{1/4}Ba_2Cu_3O_7$ HTSC and *V* is the volume concentration of $Y_3Fe_5O_{12}$ (YIG) or $Y_3Al_5O_{12}$ (YAlG).

The transport characteristics [$\rho(T)$ and I–V curves] were measured by the standard four-probe technique. The critical current was derived from the initial part of the I–V curve using the standard 1 μV/cm criterion [30]. The measurement of the transport characteristics in magnetic fields of up to 500 Oe was performed with a copper solenoid and in magnetic fields above 500 Oe, with a superconducting coil. The transport current j was passed through the sample perpendicular to the magnetic field H. The magnetic measurements were conducted on an automated vibrating-sample magnetometer [31].

3. RESULTS AND DISCUSSION

3.1. Characterization of the Composites

X-ray diffraction measurements of the $Y_{3/4}Lu_{1/4}Ba_2Cu_3O_7 + Y_3Fe_5O_{12}$ and $Y_{3/4}Lu_{1/4}Ba_2Cu_3O_7 + Y_3Al_5O_{12}$ composite samples revealed the existence of two phases only, with the 1-2-3 and garnet structures; no foreign reflections were present (within the accuracy of the x-ray analysis). The relative reflection intensities due to the $Y_{3/4}Lu_{1/4}Ba_2Cu_3O_7$ and $Y_3Fe_5O_{12}$, $Y_3Al_5O_{12}$ phases were in agreement with the volume content of the starting components in the composites. A study of the temperature dependences of the composite magnetization $M(T)$ showed the superconducting-transition onset temperature T_C to be the same for all samples, 93.5 K, which coincides with the value of T_C of the starting HTSC $Y_{3/4}Lu_{1/4}Ba_2Cu_3O_7$. The diamagnetic response decreases with increasing volume content of the nonsuperconducting component ($Y_3Fe_5O_{12}$, $Y_3Al_5O_{12}$) in the composite. Thus, x-ray diffraction and magnetic measurements permit the conclusion that HTSC-based composite materials prepared by fast sintering are indeed two-phase materials with no foreign phases present.

3.2. Transport Properties of the Composites

Figure 1 shows plots of the electrical resistivity $\rho(T)$ of the composite samples obtained in the 4.2- to 300-K temperature interval. The abrupt decrease in resistivity occurring at T_C = 93.5 K signals the transition of HTSC grains to the superconducting state. Above the transition point, the $\rho(T)$ curves are quasi-semiconducting in character. The ratio ρ(93.5 K)/ρ(300 K) grows with increasing volume content of the nonsuperconducting component in the composites. This behavior of the $\rho(T)$ relations suggests that the transport current flows through both HTSC and nonsuperconducting grains.

Below T_C, the course of the $\rho(T)$ dependences is determined by the superconducting transition in Josephson-type weak links [10, 11, 14–18]. In the reference composites HTSC + $Y_3Al_5O_{12}$, this part of the $\rho(T)$ curves exhibits a strong dependence on transport current j and external magnetic field H. Figure 2 displays $\rho(T, j)$ and $\rho(T, H)$ dependences (Figs. 2a, 2b, accordingly) obtained on the S + 15YAlG sample. We readily see that the temperature T_{C0} at which the electrical resistivity ρ becomes negligibly small ($<10^{-6}$ Ω cm) decreases as the transport current j and magnetic field H grow. This behavior of the $\rho(T, j)$ and $\rho(T, H)$ dependences is typical of the Josephson-type superconductor–insulator–superconductor (S–I–S) weak-link network; it was observed earlier on composite samples HTSC + CuO [10] and HTSC + $MgTiO_3$ [17] and has been accounted for in terms of the thermally activated phase slippage (TAPS) [32] and thermally activated vortex flow mechanisms [33]. The pattern of the $\rho(T, j)$ dependence observed in the HTSC + $Y_3Al_5O_{12}$ insulator composites under study has also been described by the TAPS mechanism [32], but its relevant analysis is beyond the scope of the present communication.

According to the thermally activated vortex flow model [33], the resistive-transition width ΔT_{C0} of S–I–S-type Josephson weak links as a function of the applied magnetic field H is defined as $\Delta T_{C0} = T_{C0}(H =$

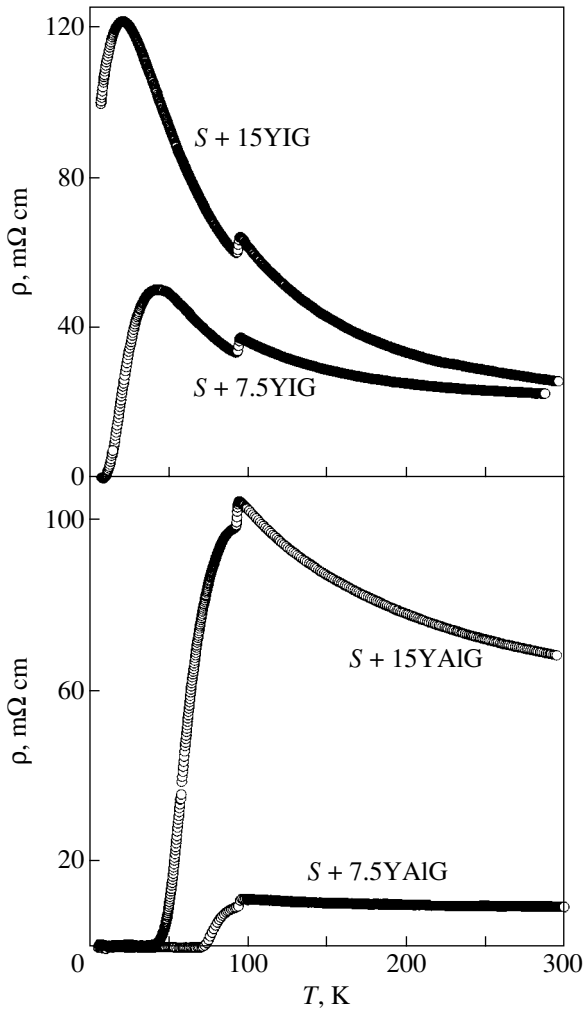

Fig. 1. Temperature dependences of electrical resistivity $\rho(T)$ of samples of HTSC + $Y_3Fe_5O_{12}$ and HTSC + $Y_3Al_5O_{12}$ obtained in the range 4.2–300 K.

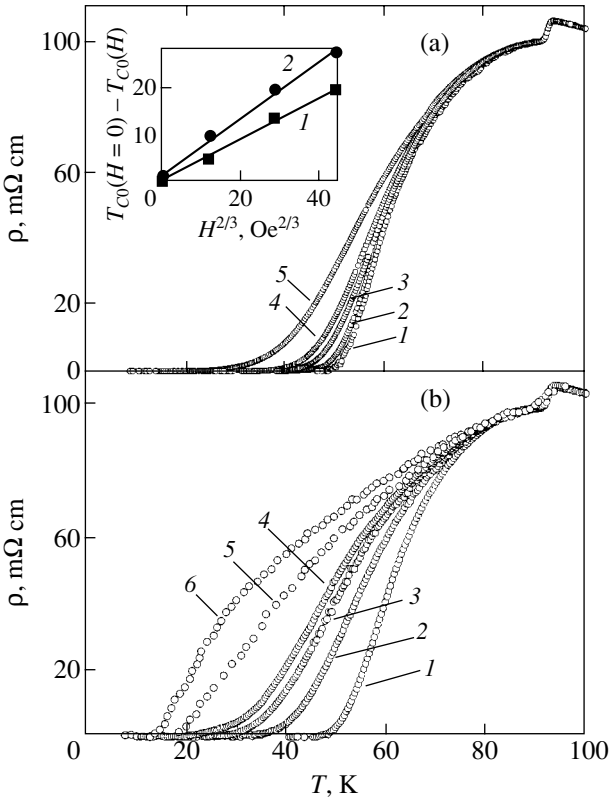

Fig. 2. Temperature dependences of electrical resistivity $\rho(T)$ of samples of HTSC + 15 vol % $Y_3Al_5O_{12}$ (S + 15YAlG) obtained at various values of (a) transport current j and (b) applied magnetic field H. (a) (*1*) j = 3.4, (*2*) 34, (*3*) 170, (*4*) 340, and (*5*) 1000 mA/cm^2; (b) (*1*) H = 0, (*2*) 37, (*3*) 150, (*4*) 292, (*5*) 2000, and (*6*) 60 000 Oe. Measuring current j = 3.4 mA/cm^2. Inset: $\Delta T_{C0} = T_{C0}(H = 0) - T_{C0}(H)$ relations plotted vs. $H^{2/3}$ for R = 0 for (*1*) S + 7.5YAlG and (*2*) S + 15YAlG.

0, R = 0) – $T_{C0}(H, R = 0)$ and scales as $H^{2/3}$. This dependence was observed experimentally on polycrystalline HTSCs [33] and HTSC + CuO composite materials [10]. The inset to Fig. 2a plots $\Delta T_{C0} = T_{C0}(H = 0, R = 0) - T_{C0}(H, R = 0)$ vs. $H^{2/3}$ for samples S + 7.5YAlG and S + 15YAlG. These dependences are seen to be close to linear in fields of up to 300 Oe. Thus, the magnetoresistive properties of the reference composites HTSC + $Y_3Al_5O_{12}$ are similar in character to those of the HTSC + insulator composites [10] and polycrystalline HTSCs [33].

HTSC + ferrimagnet composites exhibit a radically different pattern of transport properties (Figs. 3, 4). Below the temperature T_C at which $Y_{3/4}Lu_{1/4}Ba_2Cu_3O_7$ is transferred to the superconducting state (93.5 K), there is an interval in which the electrical resistivity $\rho(T)$ behaves in a semiconducting manner, as is the case above T_C. The strong dependence of electrical resistivity ρ on transport current j and magnetic field H, which is typical of a Josephson-type weak-link network, is observed only below a certain temperature T_m. The value of T_m depends on the volume concentration of the ferrimagnet in the composite, i.e., on the effective extension of weak links in space [10, 11]. For the S + 15YIG sample, we have $T_m \approx 40$ K; for S + 7.5YIG, $T_m \approx 55$ K; and for S + 3.75YIG, $T_m \approx 65$ K. The I–V curves of the samples are linear in the T_C–T_m range (Fig. 5). For the S + 15YIG sample, there is no critical current j_C at T = 4.2 K; for the S + 7.5YIG sample, j_C(4.2 K) = 0.025 A/cm^2; and for S + 3.75YIG, j_C(4.2 K) = 1.12 A/cm^2. The superconducting properties of the HTSC + ferrimagnet composites are strongly suppressed at relatively small values of the transport current and of the magnetic field. For instance, the temperature behavior of the electrical resistivity $\rho(T)$ of the S + 15YIG sample (Fig. 4) at a threshold transport current j_{cr} = 0.6 A/cm^2 (H = 0) or at a threshold external magnetic field H_{cr} = 1900 Oe (measuring current density j = 0.015 A/cm^2) continues to have the semiconducting character observed in the T_m–T_C interval.

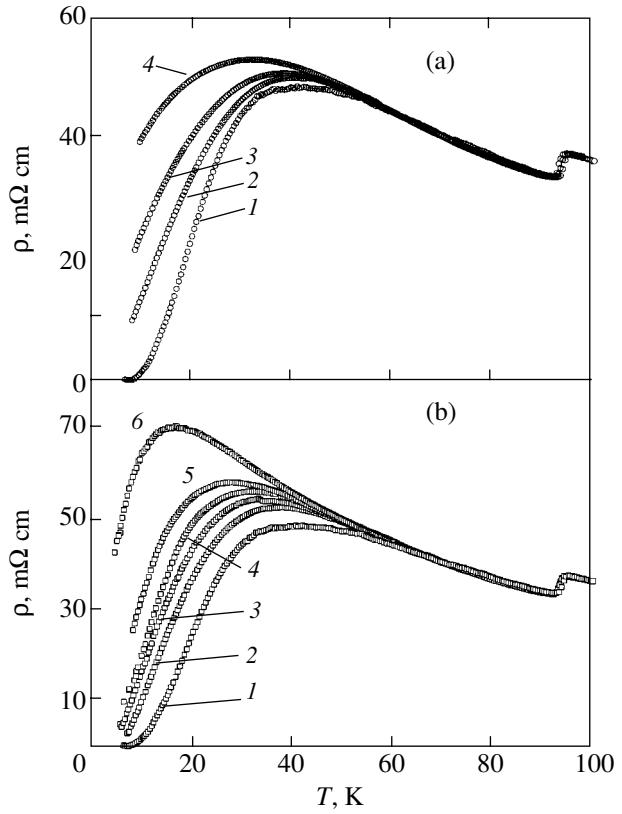

Fig. 3. Temperature dependences of electrical resistivity ρ(*T*) of a sample of HTSC + 7.5 vol % $Y_3Fe_5O_{12}$ (S + 7.5YIG) obtained at various values of (a) transport current *j* and (b) applied magnetic field *H*. (a) (*1*) *j* = 10, (*2*) 50, (*3*) 130, and (*4*) 510 mA/cm^2; (b) (*1*) *H* = 0, (*2*) 40, (*3*) 80, (*4*) 150, (*5*) 290, and (*6*) 2100 Oe. Measuring current *j* = 10 mA/cm^2.

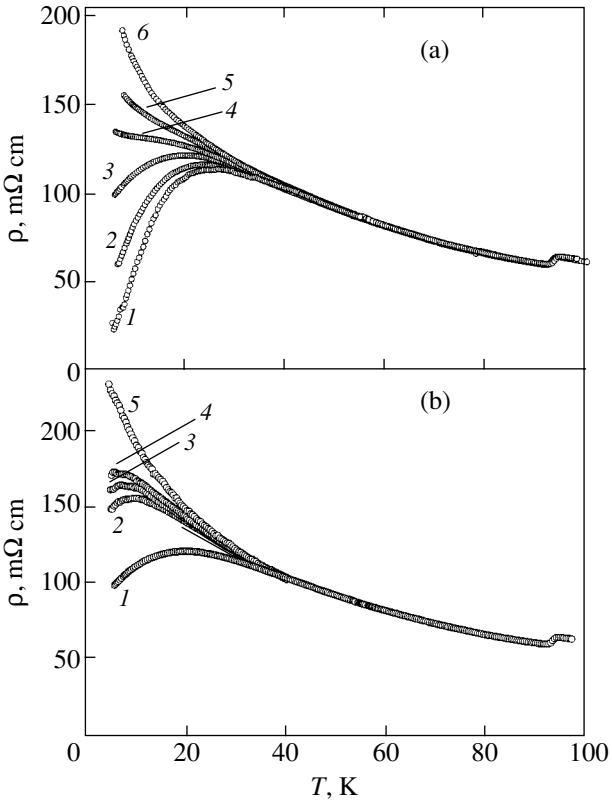

Fig. 4. Temperature dependences of electrical resistivity ρ(*T*) of a sample of HTSC + 15 vol % $Y_3Fe_5O_{12}$ (S + 15YIG) obtained at various values of (a) transport current *j* and (b) applied magnetic field *H*. (a) (*1*) *j* = 1.5, (*2*) 7.7, (*3*) 15, (*4*) 77, (*5*) 150, and (*6*) 600 mA/cm^2; (b) (*1*) *H* = 0, (*2*) 40, (*3*) 80, (*4*) 150, and (*5*) 1900 Oe. Measuring current *j* = 15 mA/cm^2.

Thus, the transport properties of HTSC + ferrimagnet composites differ radically from those of the reference composites HTSC + $Y_3Al_5O_{12}$ nonmagnetic insulator. The data presented in Figs. 1, 3, and 4 show that the *I–V* curves of the HTSC + ferrimagnet Josephson junction network are nonlinear only in the temperature interval below T_m, whereas for the reference composites HTSC + $Y_3Al_5O_{12}$ the *I–V* curves remain nonlinear up to T_C.

We believe that this effect cannot be due to the nonsuperconducting boundaries being distributed in thickness or to the technology of preparation of the composites, because the magnetoresistive properties of the reference composites $Y_{3/4}Lu_{1/4}Ba_2Cu_3O_7$ + $Y_3Al_5O_{12}$ are well described in terms of the TAPS mechanism [32] and thermally activated vortex flow [33]. Moreover, our results correlate with the data obtained in a study [27] of single superconductor–ferromagnet–superconductor Josephson junctions, where niobium served as the superconductor and gadolinium, as the ferromagnet. The ρ(*T*) dependences of a single Nb/Al/Gd/Al/Nb Josephson junction reported on in [27] also exhibit two different regions below the T_C of niobium (≈7.6 K) separated by a temperature T_m. At temperatures below T_m, the *I–V* curves are nonlinear, while in the T_C–T_m interval the values of ρ(*T*) do not depend on the applied transport current *j*. The values of T_m are ≈5.2 K for the Gd thickness 4 nm and ≈4 K for the thickness ≈8 nm.

We propose two possible explanations to account for the unusual transport properties of the HTSC + ferrimagnet composites.

The unusual pattern of the ρ(*T*, *j*) and ρ(*T*, *H*) dependences for the HTSC + $NiTiO_3$ paramagnetic insulator composites was qualitatively interpreted in [17, 18] in terms of a hypothesis assuming the formation of an Abrikosov vortex lattice in HTSC grains. Indeed, the magnetically active component of the composite induces a certain effective field that penetrates in the form of Abrikosov vortices into the HTSC grains to the Josephson penetration depth (~1000 Å [34]). This field at the HTSC/$Y_3Fe_5O_{12}$ interface is approximately equal in magnitude to the effective field (10^6 Oe for $Y_3Fe_5O_{12}$ [35]). In flowing through the composite, the transport current inevitably crosses both the HTSC grains and the ferrimagnet. Therefore, the current should also flow through the region of the HTSC grains where the Abrikosov vortices formed. Assuming that the temperature

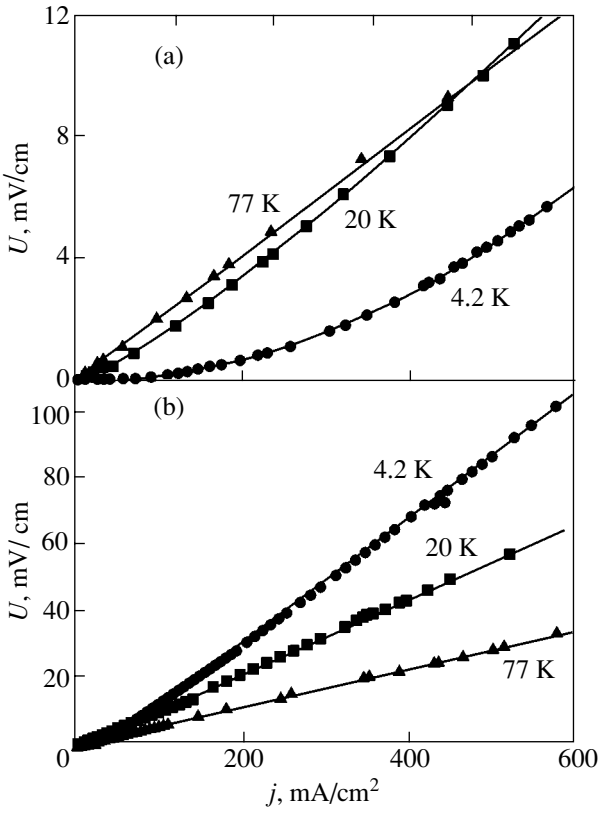

Fig. 5. *I–V* characteristics of samples (a) S + 7.5YIG and (b) S + 15YIG obtained at various temperatures.

T_m observed by us is the melting point of the Abrikosov vortex lattice, this hypothesis can account for the unusual character of the $\rho(T)$ dependences of the HTSC + ferrimagnet composites. In the T_C–T_m interval, vortices move without pinning and the resistivity does not depend on the transport current and magnetic field. Below T_m, the vortices are pinned inside the HTSC grains, which results in the *I–V* curves being nonlinear [36]. An increase in the volume concentration of a ferrimagnet in the composite corresponds to an increase in the HTSC/$Y_3Fe_5O_{12}$ interface area, which brings about an increase in the number of Abrikosov vortices and a decrease in the T_m temperature.

Another explanation of the results obtained is conceivable. A theoretical study was made in [21] of the stationary Josephson effect with ordered magnetic moments localized in the barrier. It is believed [21] that the Josephson superconducting current vanishes at a certain critical barrier thickness because of the Cooper pairs being scattered by magnetic moments in the barrier. On the other hand, the TAPS effect [32] accounts for the experimentally observed vanishing of the critical current in the S–I–S structure at temperatures close to the transition temperature of the superconducting banks due to the temperature-induced voltage fluctuations at the junction. Substitution of $I_1 = 0$ (I_1 is the critical current of the S–I–S junction in the absence of thermal fluctuations) into the expression for the *I–V* characteristic in the TAPS model [32] results in a linear $U(I)$ dependence. The vanishing of the critical current I_1 in the S–F–S Josephson junction network predicted theoretically [21] for a single junction transforms the linear *I–V* curves into nonlinear curves at the temperature T_m. Thus, theory [21] and the TAPS mechanism [32] can provide a qualitative interpretation for the $\rho(T)$ behavior of the HTSC + ferrimagnet composites. Unfortunately, theory [21] yields only a very rough estimate, because ferrimagnetic ordering is not taken into consideration. Moreover, the results obtained for HTSCs and low-temperature superconductors may differ from one another, a point mentioned in [25].

3.3. Magnetic Properties of HTSC + Ferrimagnet Composites

Figure 6 presents field dependences of the magnetization $M(H)$ of samples with different volume contents of nonsuperconducting components, namely, S + 15YIG (on the right) and S + 15YAlG (on the left) measured in the 4.2- to 100-K temperature interval. The hysteresis loops of the sample with $Y_3Al_5O_{12}$ are typical of HTSCs [34]. The $M(H)$ plots of the sample with $Y_3Fe_5O_{12}$ actually represent a superposition of hysteresis loops of the superconductor and the ferrimagnet, which is clearly seen from the $M(H)$ graphs recorded at T = 61 and 100 K (Fig. 6). Thus, magnetic measurements provide additional evidence for the existence of only two phases in the composite, namely, $Y_{3/4}Lu_{1/4}Ba_2Cu_3O_7$ and $Y_3Fe_5O_{12}$.

Figure 7 specifies the diamagnetic responses $M(H)$ obtained at T = 4.2 K from the HTSC phase in the composites S + 15YIG and S + 15YAlG. To select the diamagnetic response from the HTSC phase in a composite containing a ferrimagnet, the response due to the $Y_3Fe_5O_{12}$ ferrimagnet phase was subtracted from the integral $M(H)$ curve (Fig. 6, T = 4.2 K) with allowance for the temperature dependence $M(T)$ of this response. As seen from Fig. 7, the diamagnetic response of the HTSC phase present in the composite with the ferrimagnetic insulator (S + 15YIG) is smaller than that for the composite with the nonmagnetic insulator (S + 15YAlG). Because the technology of preparation and the volume concentrations of the components of the composites are the same in both cases, this decrease in the diamagnetic response can be accounted for by suppression of the superconducting properties in the surface layers of HTSC grains under the influence of the ferrimagnet. Indeed, the magnetically active component $Y_3Fe_5O_{12}$ of the composite induces a magnetic field, which penetrates into the HTSC grains and destroys the superconducting state.

As follows from Fig. 7, the superconductor with suppressed superconducting properties takes up 30% of the volume. Assuming the HTSC grains in the composite to have spherical shape with an average diameter of 1.5 μm (as derived from scanning electron microscopy

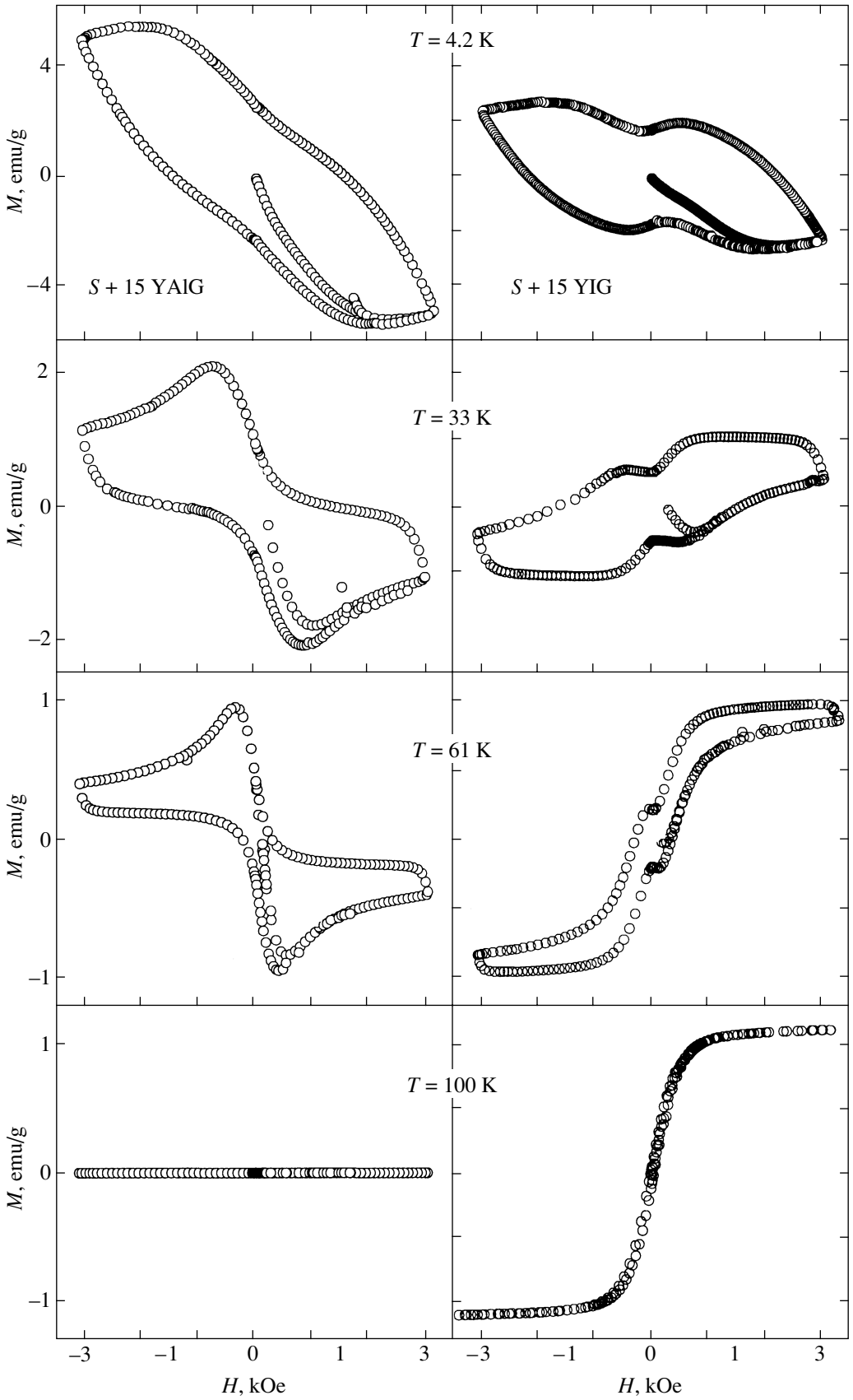

Fig. 6. *M*(*H*) plots of samples S + 15YAlG and S + 15YIG obtained at various temperatures.

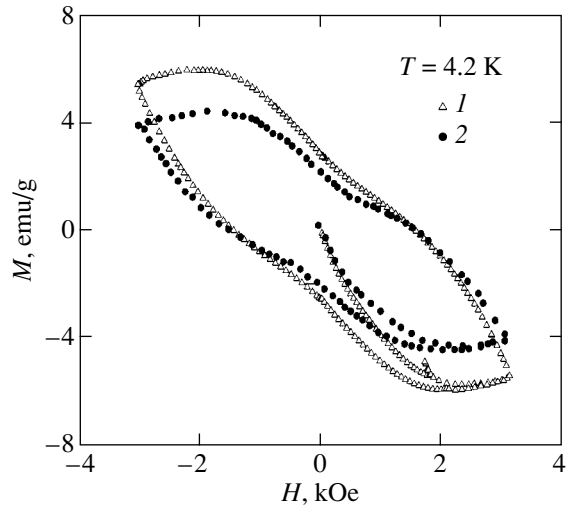

Fig. 7. Diamagnetic response $M(H)$ measured for different HTSC phases in the composites at 4.2 K. (*1*) S + 15YAlG reference composites and (*2*) S + 15YIG composites.

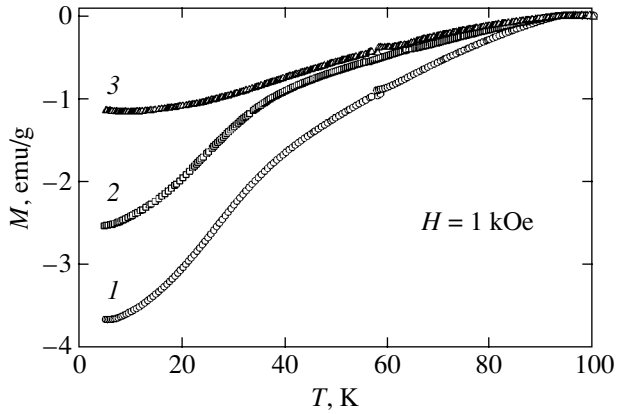

Fig. 8. Diamagnetic response $M(T)$ measured at $H = 1$ kOe for different HTSC phases in the composites. (*1*) S + 15YAlG reference composites, (*2*) S + 15YIG composites, and (*3*) difference between relations *1* and *2*.

data), estimation of the HTSC layer "suppressed" by its proximity to the ferrimagnet yields a thickness of ≈800 Å, a figure that correlates with the penetration depth of ~1000 Å for $YBa_2Cu_3O_7$ [34]. A similar estimate (≈800 Å) is obtained from the temperature dependences of magnetization $M(T)$ (Fig. 8). Figure 8 presents the diamagnetic response $M(T)$ due to the HTSC phases in the S + 15YIG and S + 15YAlG composites, as well as the difference between these curves.

4. CONLUSIONS

Thus, we have studied the transport and magnetic properties of the $Y_{3/4}Lu_{1/4}Ba_2Cu_3O_7 + Y_3Fe_5O_{12}$ composites, which represent a superconductor–ferrimagnet–superconductor Josephson junction network. Besides a strong suppression of transport properties (as compared to the HTSC + $Y_3Al_5O_{12}$ nonmagnetic-insulator reference composites), the HTSC + ferrimagnet composites exhibit radically different temperature dependences of the electrical resistivity. Below the transition temperature in the HTSC grains, the $\rho(T)$ dependence can be divided into two dissimilar ranges by a temperature T_m. At temperatures below T_m, the I–V curves of the HTSC + ferrimagnet composites are nonlinear (a feature characteristic of Josephson-type weak links), whereas within the T_C–T_m interval the behavior of $\rho(T)$ does not depend on the transport current and magnetic field. The resistive state of the HTSC + $Y_3Al_5O_{12}$ reference composites can be readily explained in terms of the thermally activated phase slippage (TAPS) mechanism [32] acting in the S–I–S Josephson junction network.

Magnetic measurements carried out on the composites showed that the diamagnetic response due to the HTSC phase in composites with a ferrimagnetic insulator is smaller than that of the HTSC phase in composites with a nonmagnetic insulator. This decrease in the diamagnetic response can be assigned to suppression of the superconducting properties of HTSC grains in a surface layer of thickness equal to the penetration depth of the magnetic field from the ferrimagnetic component of the composite.

ACKNOWLEDGMENTS

The authors are indebted to A.D. Balaev for his assistance in the magnetic measurements and to A.F. Bovina for x-ray diffraction analysis of the samples.

This study was supported jointly by the Russian Foundation for Basic Research and Krasnoyarsk Science Foundation (project Enisei, no. 02-02-97711) and the Lavrent'ev Competition for Young Scientists (grant, SD RAS, 2002).

REFERENCES

1. G. Xiao, F. H. Stretz, M. Z. Cieplak, *et al.*, Phys. Rev. B **38** (1), 776 (1988).
2. B. R. Weinberger, L. Lynds, D. M. Potrepka, *et al.*, Physica C (Amsterdam) **161**, 91 (1989).
3. J. Koshy, K. V. Paulose, M. K. Jayaraj, and A. D. Damodaran, Phys. Rev. B **47** (22), 15304 (1993).
4. E. Bruneel and S. Hoste, Int. J. Inorg. Mater., No. 1, 385 (1999).
5. D. Berling, B. Loegel, A. Mehdaouli, *et al.*, Supercond. Sci. Technol. **11** (11), 1292 (1998).
6. M. I. Petrov, D. A. Balaev, D. M. Gohfeld, *et al.*, Physica C (Amsterdam) **314**, 51 (1999).
7. D. A. Balaev, D. M. Gokhfel'd, S. I. Popkov, *et al.*, Pis'ma Zh. Tekh. Fiz. **27** (22), 45 (2001) [Tech. Phys. Lett. **27**, 952 (2001)].

8. A. G. Mamalis, S. G. Ovchinnikov, M. I. Petrov, *et al.*, Physica C (Amsterdam) **364–365**, 174 (2001).
9. J. J. Calabrese, M. A. Dubson, and J. C. Garland, J. Appl. Phys. **72** (7), 2958 (1999).
10. M. I. Petrov, D. A. Balaev, K. A. Shaĭkhutdinov, and K. S. Aleksandrov, Fiz. Tverd. Tela (St. Petersburg) **41** (6), 969 (1999) [Phys. Solid State **41**, 881 (1999)].
11. M. I. Petrov, D. A. Balaev, K. A. Shaihutdinov, and K. S. Aleksandrov, Supercond. Sci. Technol. **14** (9), 798 (2001).
12. J. Jung, M. A.-K. Mohamed, I. Isaak, and L. Friedrich, Phys. Rev. B **49** (17), 12188 (1994).
13. B. I. Smirnov, T. S. Orlova, and N. Kudymov, Fiz. Tverd. Tela (St. Petersburg) **36**, 3542 (1994) [Phys. Solid State **36**, 1883 (1994)].
14. M. I. Petrov, D. A. Balaev, S. V. Ospishchev, *et al.*, Phys. Lett. A **237** (1–2), 85 (1997).
15. M. I. Petrov, D. A. Balaev, K. A. Shaĭkhutdinov, and S. G. Ovchinnikov, Fiz. Tverd. Tela (St. Petersburg) **40** (9), 1599 (1998) [Phys. Solid State **40**, 1451 (1998)].
16. M. I. Petrov, D. A. Balaev, S. V. Ospishchev, and K. S. Aleksandrov, Fiz. Tverd. Tela (St. Petersburg) **42** (5), 791 (2000) [Phys. Solid State **42**, 810 (2000)].
17. M. I. Petrov, D. A. Balaev, K. A. Shaĭkhutdinov, and S. I. Popkov, Pis'ma Zh. Éksp. Teor. Fiz. **75** (3), 166 (2002) [JETP Lett. **75**, 138 (2002)].
18. M. I. Petrov, D. A. Balaev, and K. A. Shaihutdinov, Physica C (Amsterdam) **361**, 45 (2001).
19. L. N. Bulaevskiĭ, V. V. Kuziĭ, and A. A. Sobyanin, Pis'ma Zh. Éksp. Teor. Fiz. **25** (7), 314 (1977) [JETP Lett. **25**, 290 (1977)].
20. L. N. Bulaevskii, V. V. Kuzii, and S. V. Panyukov, Solid State Commun. **44** (4), 539 (1982).
21. S. V. Kuplevakhskiĭ and I. I. Fal'ko, Fiz. Nizk. Temp. **10**, 691 (1984) [Sov. J. Low Temp. Phys. **10**, 361 (1984)].
22. S. V. Kuplevakhskiĭ and I. I. Fal'ko, Fiz. Met. Metalloved. **62** (1), 13 (1986).
23. A. S. Borukhovich, Usp. Fiz. Nauk **169** (7), 737 (1999) [Phys. Usp. **42**, 653 (1999)].
24. M. Fogelstrom, Phys. Rev. B **62** (17), 11812 (2000).
25. Y. Tanaka and S. Kashivaya, J. Phys. Soc. Jpn. **69**, 1152 (2000).
26. Yu. Izyumov, Yu. Proshin, and M. G. Khusainov, Usp. Fiz. Nauk **172** (2), 113 (2002) [Phys. Usp. **45**, 109 (2002)].
27. O. Bourgeois, P. Gandit, A. Sulpice, *et al.*, Phys. Rev. B **63**, 064517 (2002).
28. M. Schock, C. Surgers, and H. von Lohneysen, Eur. Phys. J. **14**, 1 (2000).
29. V. V. Ryazanov, V. A. Oboznov, A. Yu. Rusanov, *et al.*, Phys. Rev. Lett. **86** (11), 2427 (2001).
30. A. Barone and G. Paterno, *Physics and Applications of the Josephson Effect* (Wiley, New York, 1982; Mir, Moscow, 1984).
31. A. D. Balaev, Yu. V. Boyarshinov, M. M. Karpenko, and B. P. Khrustalev, Prib. Tekh. Éksp., No. 3, 167 (1985).
32. V. Ambegaokar and B. Halperin, Phys. Rev. Lett. **22**, 1364 (1969).
33. M. Tinkham, Phys. Rev. Lett. **61** (14), 1658 (1988).
34. *Physical Properties of High Temperature Superconductors*, Ed. by D. M. Ginzberg (World Sci., Singapore, 1989; Mir, Moscow, 1990).
35. S. Krupička, *Physik der Ferrite und der Verwandten Magnetischen Oxide* (Vieweg, Braunschweig, 1973; Mir, Moscow, 1976), Vol. 1.
36. M. Charalambous, J. Chaussy, and P. Lejay, Phys. Rev. B **45** (9), 5091 (1992).

Translated by G. Skrebtsov